Fastener Demands for Sheathing-Braced Cold-Formed Steel Stud Gravity Walls

Abstract

We explore, in this paper, the demands and behavior on fasteners supplying sheathing-based bracing of gravity loaded cold-formed studs and wall assemblies. The studies are carried out by shell finite element (FE) models, which are compared to analytical solutions and previously completed laboratory tests conducted by the authors. The connection between the sheathing and the stud should be able to develop enough resistance to restrain global buckling of the studs; therefore, special attention has to be given to the demands on these connections for design. Local buckling and stress concentrations may damage some connections and re-distribution of forces should be ensured. Classical practice for determining fastener demand – i.e., the 2% rule – may be deficient. An analytical method developed for determining fastener demand is compared to the FE models presented in this paper; the analytical method results in a reasonable prediction of the fastener forces in wall studs.

Keywords

fastener, cold-formed steel, stud wall

Luiz Carlos M. Vieira Junior [a]
Benjamin W. Schafer [b]

[a] University of Campinas,
email: vieira@fec.unicamp.br
[b] Johns Hopkins University,
email: schafer@jhu.edu

1 INTRODUCTION

Cold-formed steel may be used to frame the walls, floors, and roofs of modern buildings. The individual cold-formed steel members (studs) have sheathing attached to provide appropriate architectural enclosures. This sheathing also serves to brace the cold-formed steel studs under load. Current design methods are highly developed regarding the design of isolated cold-formed steel members such as columns and beams, but cold-formed steel wall studs that rely on sheathing for bracing are not fully addressed.

Significant work has been conducted on sheathing-braced cold-formed steel stud walls, Okasha (2004), Fiorino et al. (2007), and Chen et al. (2006) have concentrated their efforts in determining the resistance of the stud-to-sheathing connection; while Miller and Pekoz (1993), Winter (1960), and Simaan and Pekoz (1976) have explained their implications on the wall stud resistance, but few

have specifically investigated fastener demands. The commentary of AISI-S211 (2007), based on the research conducted by Winter (1960), states that a fastener-sheathing assembly shall be designed for a load equal to 2% of the axial load, also know as "2% rule".

It is involved to determine fastener demand experimentally; not only is it difficult to instrument fasteners and sheathing, but also each connection would have to be instrumented individually. For the reasons mentioned above, a shell FE model was developed. In the FE models we can easily analyze each demand on the fastener – lateral, axial, and rotational – separately, which facilitates the understanding of the forces developed in the connections as they attempt to brace the stud under applied gravity load.

2 FE MODELS

2.1 Single-Column FE Model

Fastener demands are explored by means of shell FE models developed to be similar to previously conducted sheathed single-column tests and sheathed wall-stud assemblies, Simaan and Pekoz (1976) and Vieira et al. (2011) and . As in the tests, all the models simulate 362S162-68 studs and 362T125-68 tracks, AISI S200 (2007). The single-column model and full wall-stud models share many modeling characteristics, such as: element type, stress-strain curve for the material, boundary conditions and initial imperfections, but they are different in terms of geometry. The single columns are 2.44m (8ft) long connected on both ends to a 0.61m (2ft) track, the sheathing is also 2.44m (8ft) long but is only 0.46m (18in) wide and it is connected to the stud every 0.30m (12in), while it is connected at every 0.15m (6in) to the track. We modeled a 2.44x2.44m (8x8ft) (two sheathing 1.22x2.44m (4x8ft) on each side) wall-stud, with 5 studs connected to the track on their ends, studs are connected to the sheathing at every 0.30m (12in) on the field and every 0.15m (6in) on the edges of the sheathing. In the tests, the studs are loaded through a loading plate 0.3m (12in) long and 0.10m (3.6in) wide to insure that only the stud is engaged in direct bearing and never the The models are built in ABAQUS (2007), using S4R[1] shell elements to model stud, track and sheathing. The material steel is simulated using the stress-strain curves depicted in Figure 1, which are transformed from engineering stress to true stress[2] for use in ABAQUS (2007). The material model chosen to represent the steel is non-linear, and it considers metal plasticity (von Mises yield surface) and isotropic hardening. The sheathing is modeled as an orthotropic material with Young's modulus (E) and shear modulus (G) as discussed in Vieira (2011) (OSB – E=6,426 MPa (932 ksi), shear G=1,310 MPa (190 ksi), thickness=7/16in; Gypsum – E=993 MPa (144 ksi), G=552 MPa (80 ksi)), thickness=1/2in and ν=0.3. The modified Riks method is used to solve the nonlinear model.

---

[1] S4R elements are used rather than S4R5, because S4R elements allow the rotation on plane of the element to be restricted.

[2] Engineering strain (ε_0) is transformed to true strain (ε) by the relationship $\varepsilon=\ln(1+\varepsilon_0)$, thus by assuming a material incompressible the true stress is given by $\sigma=\sigma(1+\varepsilon_0)$.
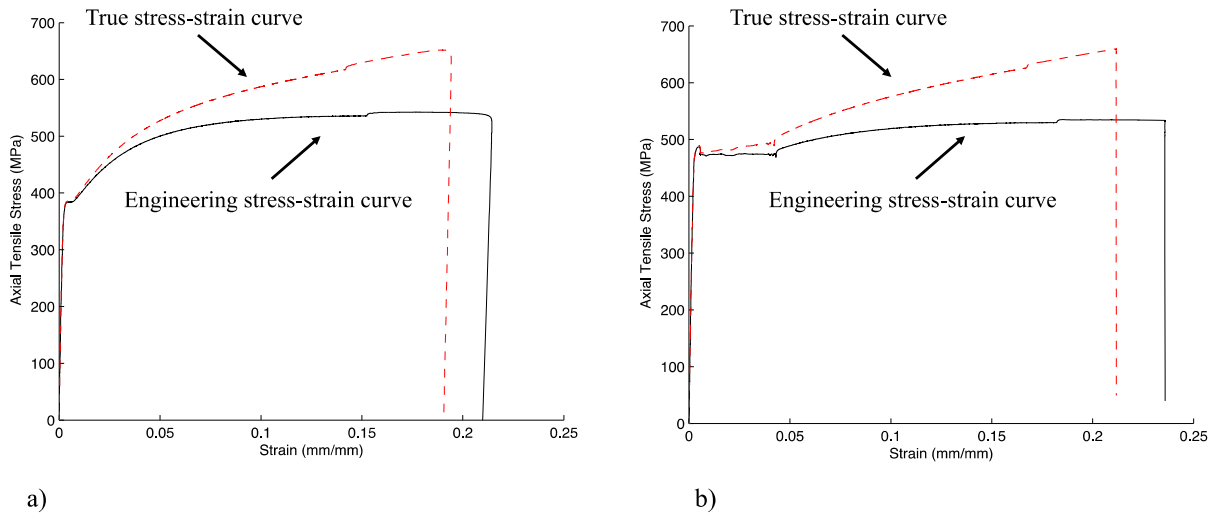
Figure 1: Stress-strain curve used for simulating: a) stud and b) track.

The stud-to-track fasteners are idealized by coupling all the degrees of freedom except the rotation around the axis of the fastener and the stud-to-track contact is idealized by coupling all the displacements except the displacement on the plane of the track's web (stud end is free to slide). A displacement is applied to a master node that transfers this displacement to a rigid body that represents the isolation plate on the track web used to load the stud.

The models have their geometry altered by an initial imperfection, which is considered as either a small initial imperfection (25th percentile) or a large initial imperfection (75th percentile). The magnitude of the initial imperfection is depicted in Table 1 and it follows Schafer and Pekoz (1998) regarding local imperfections ("d1" and "d2") and Schafer and Zeinoddini (2008) regarding global imperfections (bow, camber and twist).

Reference	Type of imperfection	$P(\Delta < d)$*	
		25th %ile	75th %ile
Schafer and Peköz (1998)	Local (d_1/t)	0.14	0.66
	Distortional (d_2/t)	0.64	1.55
Schafer and Zeiniddini (2008)	Bow	L/4755	L/1659
	Camber	L/6295	L/2887
	Twist	0.46⁰	1.23⁰

* "Probability that a randomly selected imperfection value, Δ, is less than a discrete deterministic imperfection, d." Schafer and Pekoz (1998).

Table 1: Imperfection applied on studs.

The bracing restrictions provided to the stud can be simulated with or without the sheathing in the FE model. If the sheathing is not considered in the model, the springs are connected on one end to the node where there is a fastener on the stud and the other end to a fixed support, see Figure 2

for example and for spring orientation. For models in this case the diaphragm stiffness (k_{xd}), the rotational stiffness provided by the sheathing (k_ϕ), and the out-of-plane stiffness (k_y) are However, if the sheathing is being included directly in the model, the same three variables are not considered since the sheathing is in place and it will automatically take in account these stiffnesses. The stiffness provided by the sheathing in the axial direction may also be considered and since is no specific value for k_z and $k_{\phi x}$, we have used the same values of k_x and k respectively, which in fact is a lower-bound value for these stiffnesses, Table 2.

Sheathing Material	Spring	Sheathing in place, springs idealize just the fastener	No sheathing, springs idealize fastener and sheathing
OSB	$K_x=K_z$ (N/mm)	1241	971
	K_y (N/mm)	N/A	0.374
	$K_\phi=K_{\phi x}$ (N.mm/rad)	136660	95309
Gypsum	$K_x=K_z$ (N/mm)	426	427
	K_y (N/mm)	N/A	0.087
	$K_\phi=K_{\phi x}$ (N.mm/rad)	129745	95987

Table 2: Spring stiffness used in the FE models (fastener spacing considered is 305mm (12in)), Figure 2 depicts the spring orientation. See Vieira and Schafer (2013). For more information about how to determine the springs' stiffnesses.
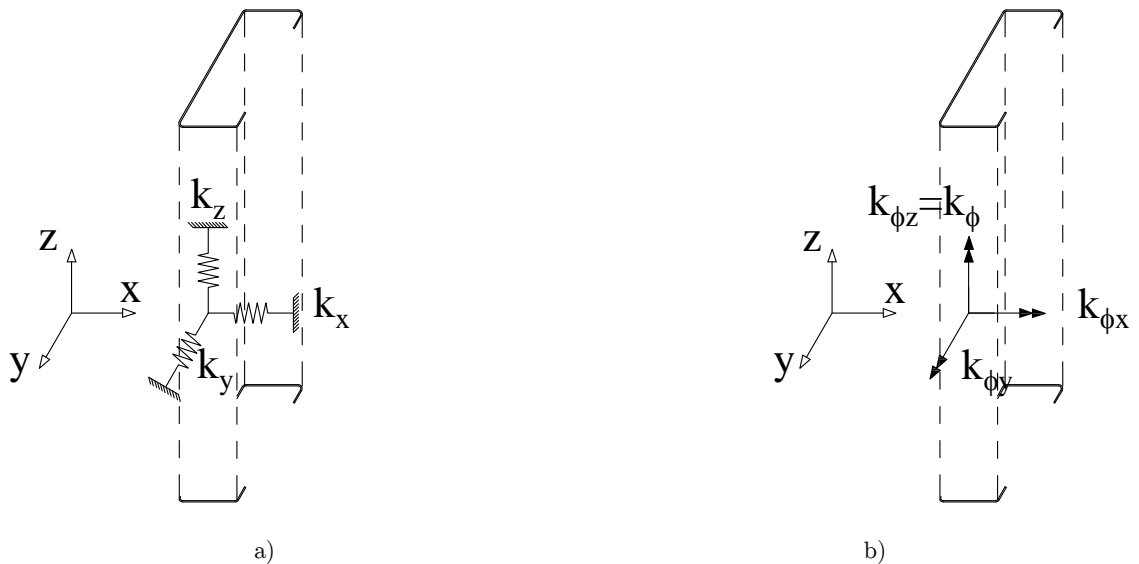

a)   b)

Figure 2: Springs orientation a) Translational springs, b) Rotational springs (only the reaction vector is plotted since the actual rotational spring drawing may confound the reader).

A series of shell FE collapse models (i.e. geometric and material nonlinear models with imperfections) for the sheathed single-column tests with varying degree of sophistication are summarized in Table 3. The first set of FE models presented compares the end boundary conditions in the models to the Bare-Bare (denotes that no sheathing was present on either flange face of the test) single-column test, 2.44m (8feet) long, Table 3. The model that simulates stud and track when compared to a column with fixed-fixed ends did not show a great difference, and both models represent a slighter higher peak than found in the test reported in Vieira and Schafer (2013). Our idealization of a boundary condition that directly couples nodes instead of using contact elements leads to a slighter stiffer system, but the presence of the track is important to establish the connection between sheathing and track, which, as it will be shown further, develops an important role in distributing the load to the stud and at the same time bracing it.

The second set of models concentrates on understanding the springs that should be considered in order to simulate the tests (this all without considering the sheathing explicitly, bot now considering tests with sheathing-bracing). In these models we found that if we only consider the springs k_x, k_y and k_ϕ, the models lead to a peak load around 16% lower than the peak load in the test, Table 3. However if we add k_z and $k_{\phi x}$, which are responsible for the contribution of the sheathing in the longitudinal direction of the stud, the results are in excellent agreement with the test. Suggesting modest composite action is present even though the vertical load is isolated.

The third set of models also compares the same single-column test (OSB-OSB, 2.44m (8feet)) to the tests, but this time the sheathing is explicitly modeled (instead of smeared into a spring stiffness); thus the spring stiffness is changed as discussed above and provided in Table 2. In the first model, instead of using springs, we coupled the displacements at the stud and track to the sheathing, which created an upper bound value for the peak loads (70% higher that the test). When we actually modeled the stud and track connected to sheathing through spring elements we found a peak load only 7% lower than found in the tests, which we consider a good prediction. Also simulated (an addendum to the third set of models) was analysis considering a linear elastic steel material: our goal with this model is to understand the fastener forces in the model if there is no plastic deformation in place. In the case of the single-column models the difference in the fastener forces are small, but the same is not observed in the wall-stud model, because in the latter model plasticity of the stud-to-track connection plays an important role.

The last set of models simulates the sheathed wall-stud test. If the springs are considered as the elements connecting the sheathing to the wall-stud, the model reaches peak load mainly due to plastic failure at the connection of stud-to-track at a load 22% lower than the test. In fact, in Vieira and Schafer (2013) tests, failure at the stud-to-track connection was not observed; perhaps a finer mesh at the stud-to-track connection could prevent the model of reaching peak load at an early stage due to the plastic failure. Nonetheless, the most important fact is that we can already see in the model an eminent local buckling failure at the stud ends, which was the same failure type seen in the test. Also, if local buckling is the dominant failure mode, it means that the springs are able to restrain global buckling, which is our main concern. Thus, we considered this model of the sheathed wall-stud suitable for the fastener force study, its primary purpose.

Configuration	Is the sheathing being model	Characteristics	Imperfection (%ile)	Peak Load (kN)	Test peak load (kN)
Bare-Bare Single Column	No	No Track / Fixed Ends	25th	71.6	57.1
		Stud + Track	25th 75th	69.1 58.2	
OSB-OSB Single Column	Yes	Springs (k_x,k_y,k_ϕ)	25th 75th	89.5 86.6	102.7
		Springs (k_x,k_y, k_z, k_ϕ,$k_{\phi x}$)	25th 75th	105.0 107.5	
		Instead of springs the nodes where coupled	75th	174.5	
		Springs (k_x,k_z, k_ϕ,$k_{\phi x}$)	25th 75th	95.8 95.6	
		Springs (k_x,k_z, k_ϕ,$k_{\phi x}$), but steel material is linear elastic	75th	173.9	
OSB-OSB Wall		Springs (k_x,k_z, k_ϕ,$k_{\phi x}$)	75th	392.4	479.5
		Springs (k_x,k_z, k_ϕ,$k_{\phi x}$), but steel material is linear elastic	75th	1934.4	

Table 3: FE models results.

A closer look into the models leads to several conclusions regarding the fastener forces (i.e. the forces at the fastener locations that supply bracing to the stud). The first model to be analyzed in depth is considered the simplest model of this series, which considers only the springs k_x, k_y and k_ϕ, and the board is not explicitly modeled, Figure 3. Figure 4 depicts the force and moments in the springs for different initial imperfections, different sides where the sheathing is connected (side 1 and 2), and different positions: ends (first spring on the stud, 50.8mm (2in) from the end), and center of stud. Local and distortional buckling are modestly affected by the presence of springs, but the springs play an important role in restricting global buckling, that includes: weak axis buckling and flexural-torsional buckling. This simple model shows that at peak load the forces on the k_x springs are at its maximum magnitude at the center of the stud, but after peak load due to local buckling, the maximum force in the springs are transferred from the center to the ends, where local buckling happens: Figure 3 (b, c). It is also shown in Figure 4 that for a 75th percentile magnitude of initial imperfection the fastener force is higher than a 25th percentile of initial imperfection (as expected); therefore, further studies are based on models that have its geometry altered by a 75th percentile initial imperfection – i.e., a plausible worst case scenario. Another conclusion is that the force at the k_y springs are very small, this is explained by the nature of the problem, since strong-axis buckling is not a predominant buckling mode it takes little resistance to restrict this direction. The moment

in the rotational spring is also very small compared to the capacity of the connection, in the tests reported in Vieira and Schafer (2013). the maximum moment at the k_ϕ spring for OSB is on the average 47.45kN.mm (420lbf.in (351lbf.in/in*12in)) while in the models the maximum moment at the spring is of 3kN.mm (26.55 lbf.in).
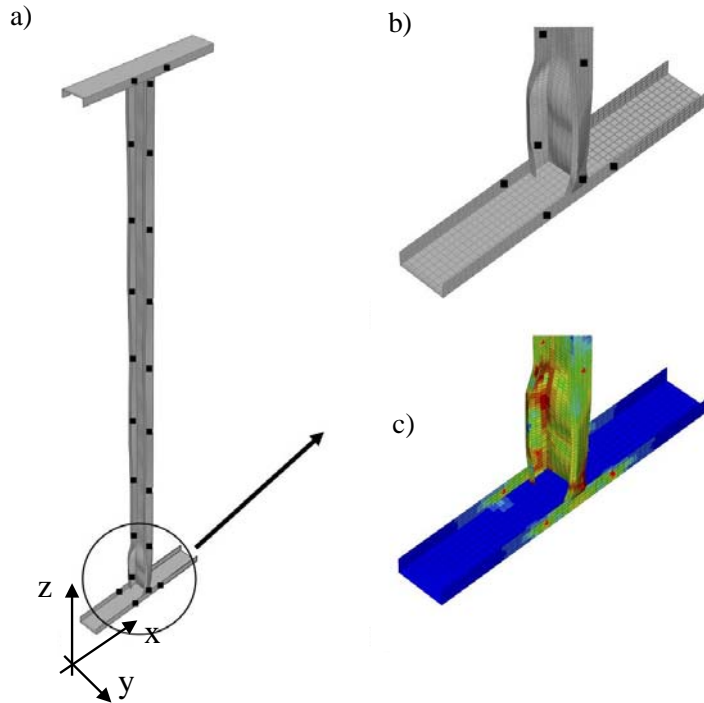

Figure 3: Simple model that considers only k_x, k_y, k_ϕ, and sheathing is simulated by means of springs
a) Single-column model, springs are depicted in black dots, b) Zoomed view of stud end where local
buckling takes place, c) von-Mises stresses on stud end.

Another single-column model interesting to explore is the one that considers k_x, k_z, k_ϕ, $k_{\phi x}$, and the sheathing, Figure 5. Figure 6 depicts the force and moment in the springs at peak load for the model of Figure 5. The demands on side 1 and 2 are plotted in different colors, but since the single-column model presents a symmetric behavior regarding the sides, the plots of side 1 and 2 are always superimposed and little difference can be seen. In the tests reported Vieira and Schafer (2013). , the average peak load carried in the translation test is 2.58kN (0.58 kips), therefore the demand in the translational springs should not exceed the peak load reported in the tests, as it is observed in Figure 6 (a, b) in the value of the maximum force. The k_x spring has the greatest magnitude close to the ends where the stud buckles in a local mode, Figure 5 (c, d). While the k_z spring has more demand at the track-to-sheathing connection and stud end, because the axial force is transferred from the loading plate to the steel members and then to the sheathing; in the middle, the applied force is counterbalanced by the reaction force and so the fasteners receive little if any load. Even though the rotational spring also has small demands, it is interesting to track their behavior. The

kφ spring has greatest demands in the middle of the stud. This shows that the kφ spring is providing a small contribution to restrain flexural-torsional buckling. Nonetheless, the kφx springs have their greatest demands at the ends, showing that the kφx springs help restrain the stud in strong-axis buckling. The primary conclusion with this model is that the group of springs and the sheathing are able to restraint global buckling and hence the stud buckles in local buckling.
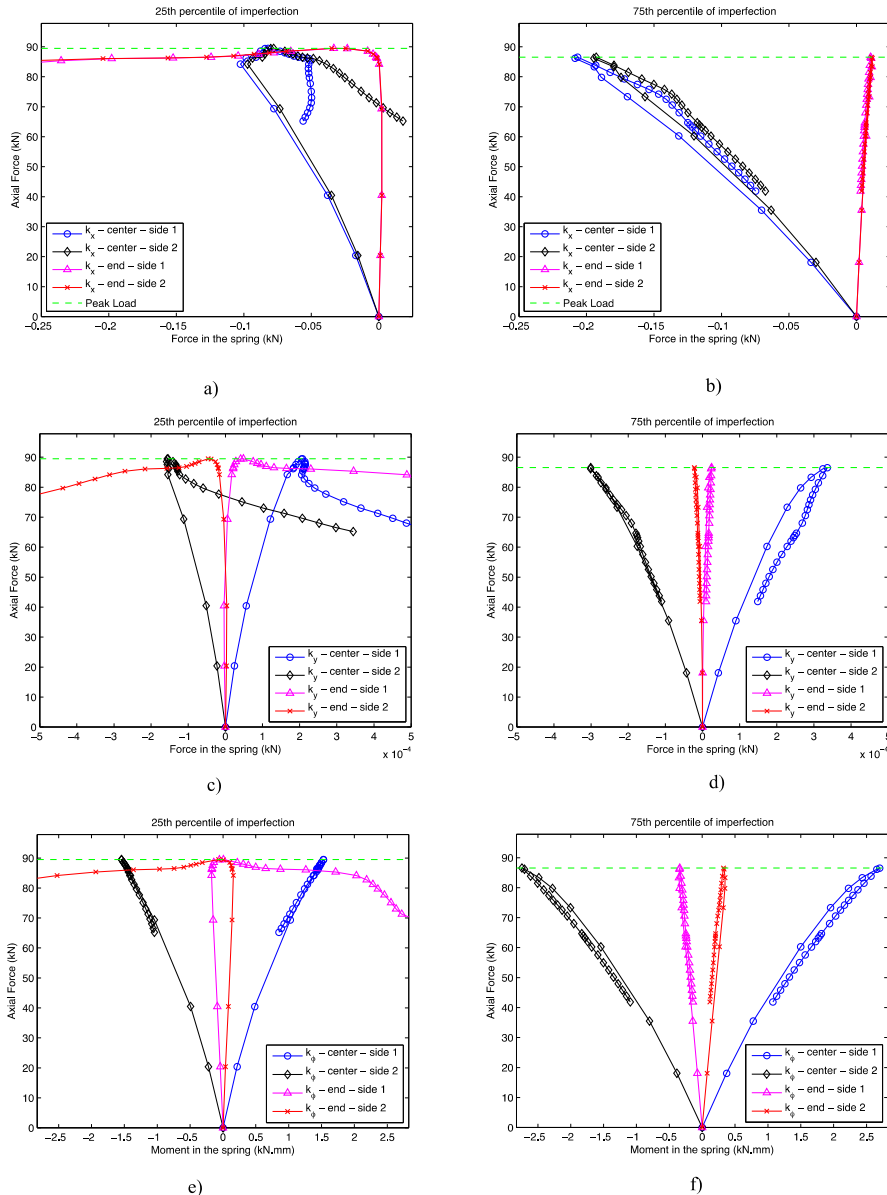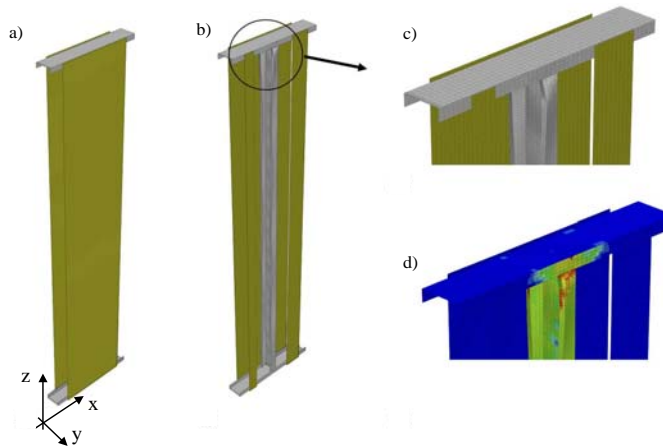

Figure 4: Simple model that considers only k_x, k_y, $k_φ$, and sheathing is simulated by means of springs a) Single-column model, springs are depicted in black dots, b) Zoomed view of stud end where local buckling takes place, c) Von-Mises stresses on stud end.

Figure 5: Model that considers k_x, k_z, $k\phi$, $k\phi x$, and sheathing is also simulated a) Overall view of FE model, steel members are represented in gray and OSB in brown, b) Part of the sheathing is removed to show the stud, d) Zoomed view of stud end where local buckling takes place, c) von Mises stress on stud end.
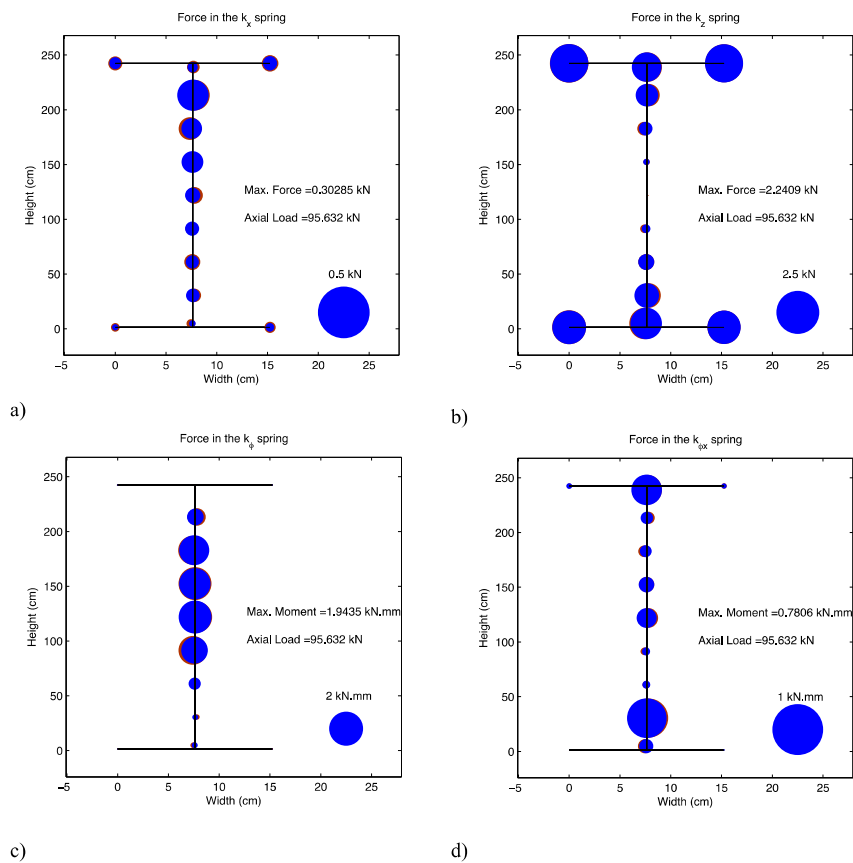

Figure 6: Force and Moment in the springs at peak load for model that considers k_x, k_z, $k\phi$, $k\phi x$, and sheathing is also simulated; initial imperfection of 75th percentile.

2.2 Full Wall Stud FE Model

2.2.1 Wall Stud Sheathed with OSB on Both Sides (OSB-OSB)

While the single-column models show perfect symmetry and a very predictable behavior, the full wall-stud model opens a new horizon to be explored; in fact, an asymmetric horizon replete with load re-distribution. It is worth recalling that the steel members on the edges (studs and tracks) are connected to sheathing every 152mm (6in.), the field studs are connected to sheathing every 254mm (12in.), and the stud in the middle that is connected to two sheathing boards is connected by two lines of fasteners (one line each board), every 152mm (6in.). The full wall shell FE model is depicted in Figure 7.
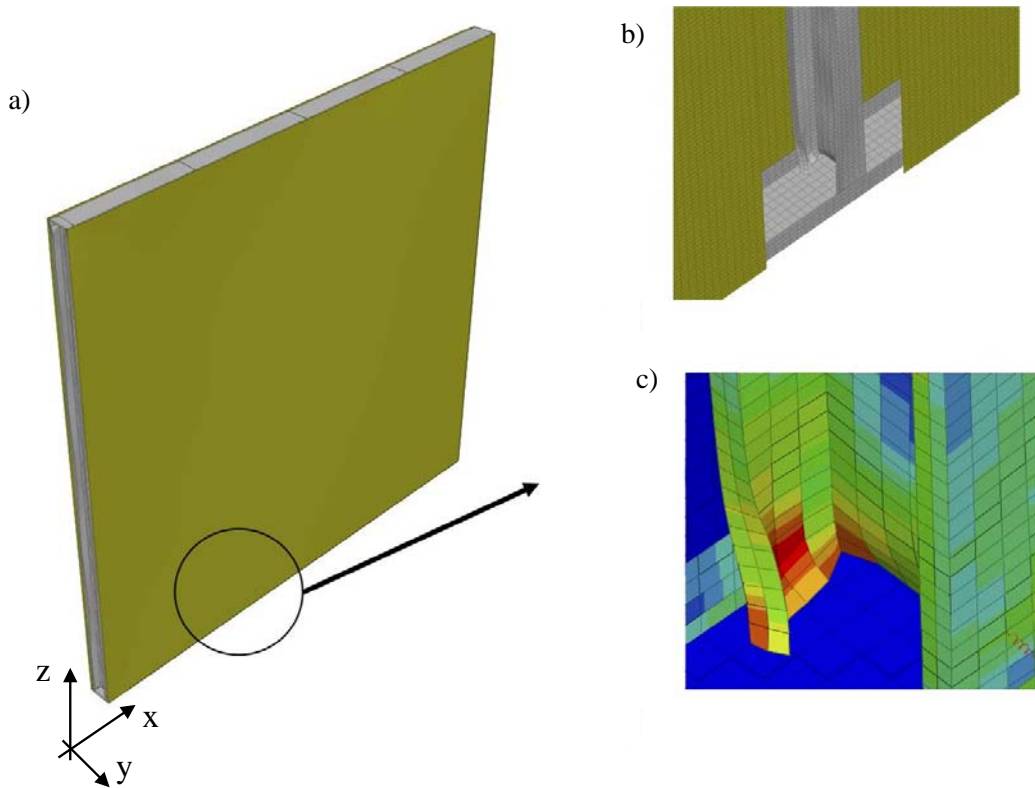

Figure 7: FE Model considers k_x, k_z, $k\phi$, $k\phi_x$, and sheathing is also simulated (OSB-OSB) a) Overall view of FE model, steel members are represented in gray and OSB in brown, b) Zoomed view of stud end where local buckling takes place, the sheathing is partially removed to provide view of the stud, c) von Mises stress on stud end, special attention is brought to the stud-to-track connection where plastic failure takes place.

The k_x spring has highest demands at the ends, where the stud is undergoing local buckling. At the peak load, the corners are the places that the springs present the highest demands, Figure 8(a). The k_x spring is explored in more detail in the following. The k_z spring reaches its full capacity (2.58kN (0.54kips)) at the bottom track, Figure 8(b). This happens because the stud-to-track connection is undergoing local plastic failure, Figure 8(c), and the sheathing is responsible for transferring the load to the stud. As in the single-column models, the rotational springs demonstrate small

load levels compared to their resistance, but are still important for understanding the whole behavior of the system, Figure 8(c, d). The higher loads in the $k_{\phi x}$ spring are at the end of the studs and track, implying that $k_{\phi x}$ helps restrain flexural-torsional buckling of the stud and bending of the track flanges. But k_ϕ loads are higher at the edge studs; due to the asymmetric contribution of the sheathing to the stud. At the edges, the flange of the stud is responsible for anchoring the sheathing that is bending out of its plane, while at the other studs the bending moment is counterbalanced by the continuation of the sheathing.
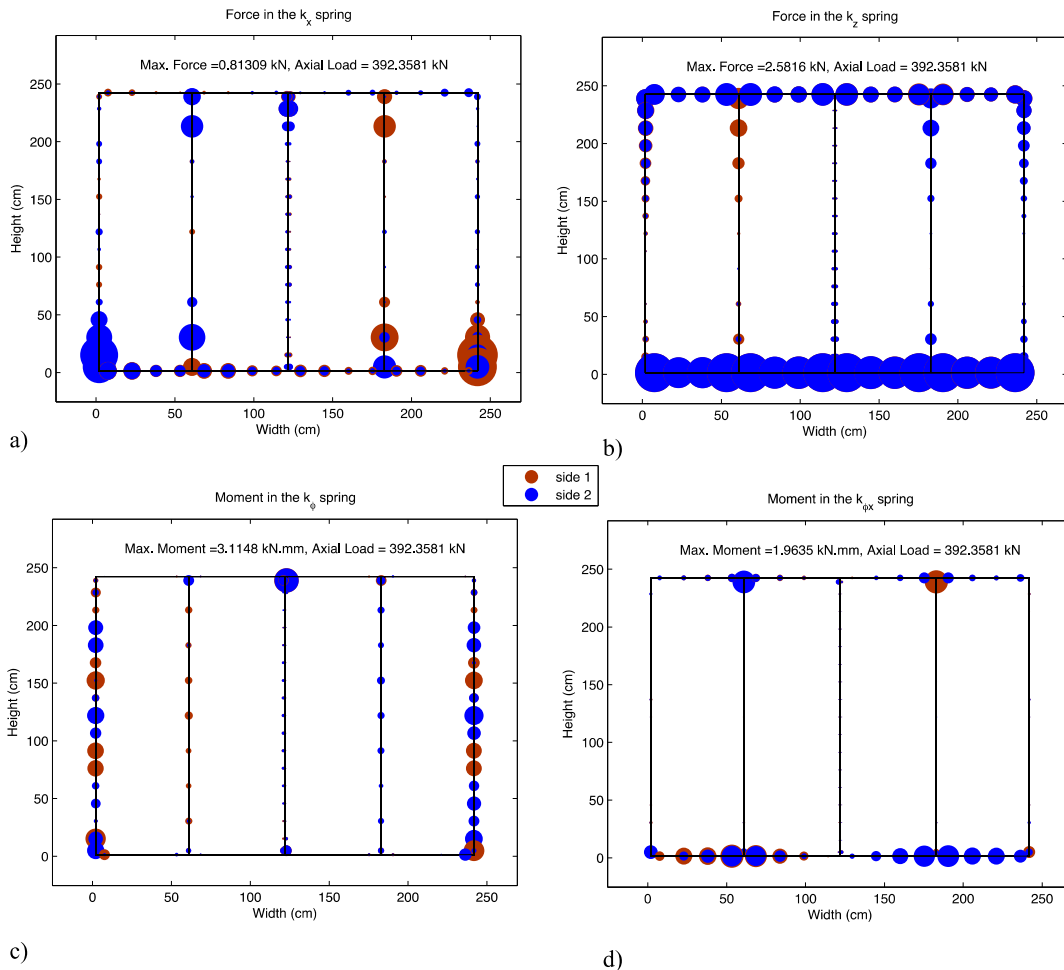

Figure 8: Force and Moment in the springs at peak load for non-linear sheathed wall-stud model (k_x, k_z, k_ϕ, $k_{\phi\xi}$) (OSB-OSB). The biggest marker is equivalent to the maximum moment or force of each picture.

Special attention is warranted for the k_x spring (Figure 9), which is the spring (bracing direction) most responsible for restraining global buckling and therefore beneficially driving the stud to fail in a higher local buckling mode The first thing that is brought to attention is the asymmetric character of the force distribution. The asymmetry of the sheathing contribution to brace the stud

defines the side that has greatest demands. For example, the second stud from left to right has a sheathing contribution from the right side of the stud higher than from the left side and thus the spring on side 2 receives more load than side 1, and the problem is inverted on the fourth stud and thus the spring that receives more load is on side 1. However, if both plots are superposed as in Figure 8(a) the overall load plot is symmetric. Another interesting observation is the force distribution in k_x over different load steps. Until about 85% of the peak load, Figure 9(a, b), the studs that has higher loads in the springs are the field studs (second and fourth studs), and this is due to the development of local buckling at the end of those studs, Figure 7(b), but after 85% of peak load the force on the field studs does not increase and the connections in the corners start taking more lateral load. There is always some doubt about what is the least favorable situation: higher fastener spacing (field studs) or less sheathing contribution (edge studs). This study shows that the sheathing may be able to redistribute the loads and balance either the lower number of fasteners or the smaller effective width of the sheathing, but the redistribution depends on the extent to which local buckling is developed at the ends of the field studs.
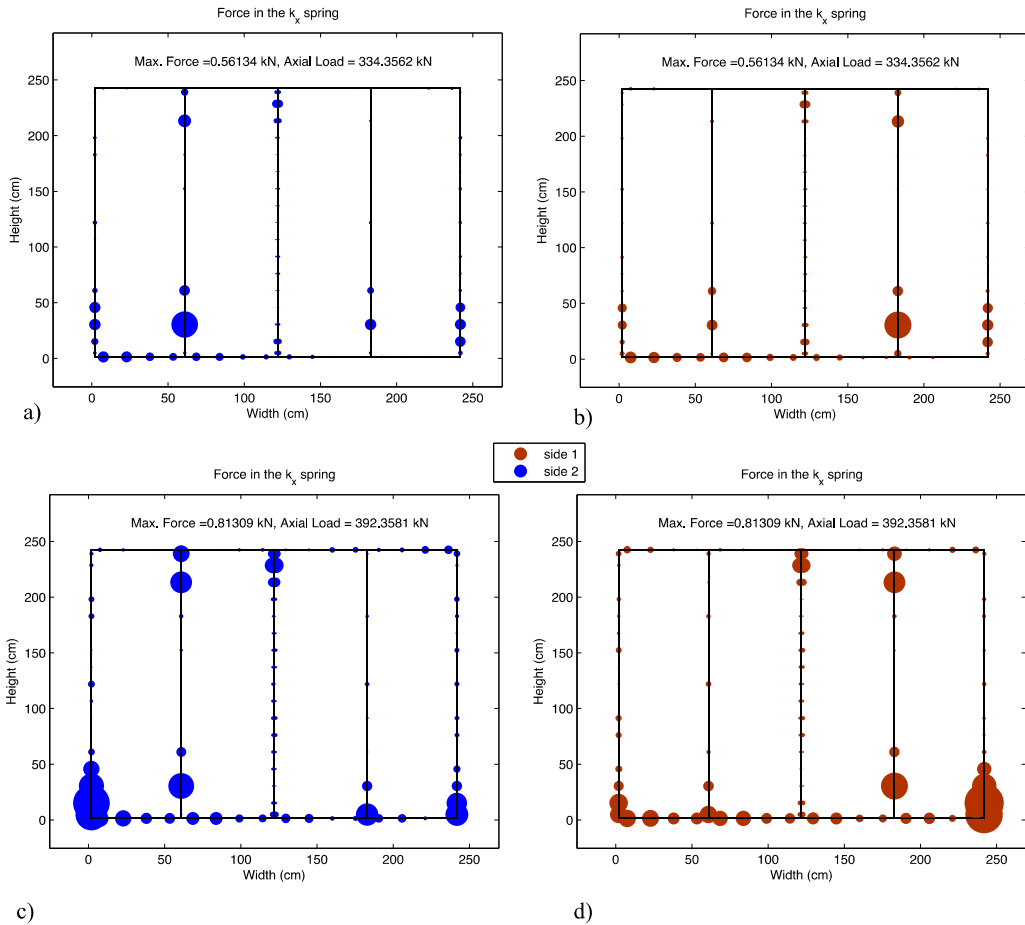

Figure 9: Distribution of the forces in the k_x springs varying side that is being attached and axial load (OSB-OSB wall). The biggest marker is equivalent to the maximum moment or force of each picture.

2.2.2 Wall Stud Sheathed with OSB on One Side Only (OSB-BARE)

Another interesting case to be explored is a wall stud sheathed with OSB on one side only (OSB-BARE), Figure 10. There is some concern that since the studs failed in flexural-torsional buckling during the tests the fastener demand on walls with studs sheathed on one side only would be bigger than walls sheathed on both sides. The models actually show that the fasteners demands in OSB-BARE walls are lower than in OSB-OSB walls, see Figure 10 and Figure 11, which correspond well to what was seen in the tests. In the OSB-BARE tests the connections were not fully damaged after peak load; however in OSB-OSB tests the connections were fully damaged, especially close to the ends where local buckling takes place. Although the OSB-BARE condition is not a beneficial one in terms of strength, it is not observed to be problematic in terms of bracing demands developed in the stud to sheathing fasteners.
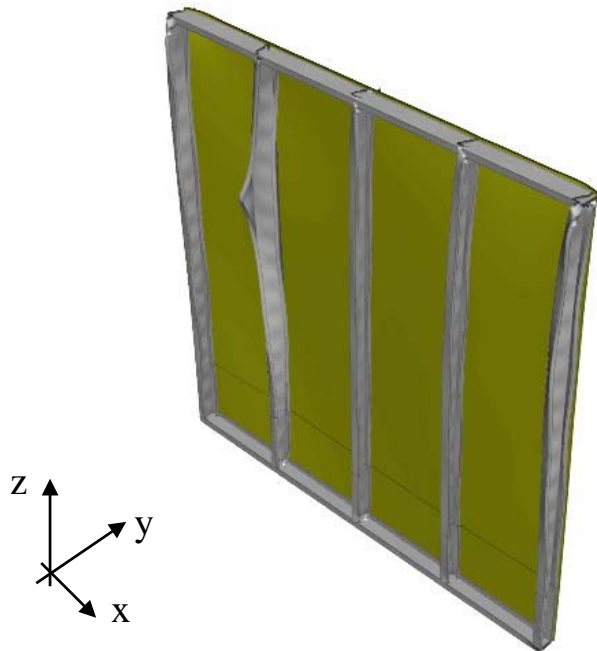

Figure 10: FE Model considers k_x, k_z, $k\phi$, $k\phi_x$, and OSB sheathing on one side only.

The k_x springs have the greatest demands at the stud that buckles first – second stud (left to right). Unlike in the OSB-OSB model, the force doesn't redistribute to the edge studs, although the k_x springs at the edge studs still play an important role in bracing the wall, as can be observed by the amount of force in the k_x springs at the edge studs, see Figure 11(a). The k_z springs follow the same load distribution as in the OSB-OSB walls. The $k\phi$ springs have greater demand than the OSB-OSB case, since the studs are buckling in flexural-torsional buckling and the $k\phi$ spring attempts to restrain torsion of the stud. The moment magnitude at the $k\phi_x$ spring is slightly affected

by the sheathing asymmetry, Figure 11(d), but the moment resisted by the spring looses its symmetry as depicted in Figure 8(d).
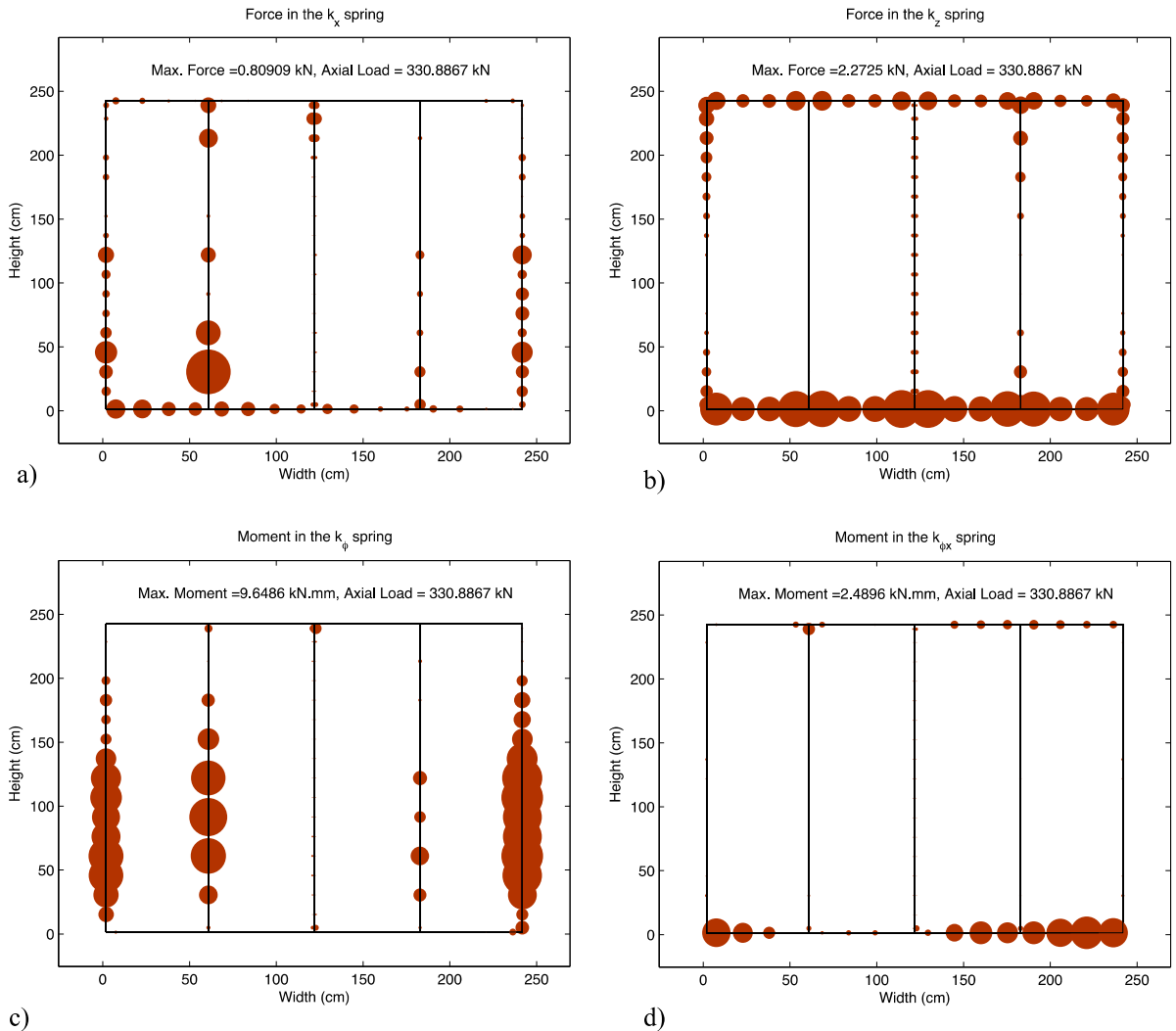

Figure 11: Force and Moment in the springs at peak load for non-linear sheathed wall-stud model (k_x, k_z, $k\phi$, $k\phi\xi$) (OSB-BARE). The biggest marker is equivalent to the maximum moment or force of each picture.

2.3 Necessary Strength of Connections

The 2% bracing rule has been used to imply that if the fasteners are designed such that the sum of the forces on the fasteners is at least 2% of the axial load they should provide adequate bracing. This empirical rule has been used implicitly or explicitly since 1962 by the cold-formed steel design codes[3]. In 2008 Schafer et al. (2008) showed that following the assumptions established by Winter

---

[3] For flexural buckling only AISI-S100 (2007) adopted a more modern strength and stiffness requirement.

(1960) the actual necessary bracing force is in fact 1% of the axial load, therefore the design codes in essence adopted a safety factor of 2. The 2% rule can be compared against the FE models. Figure 12 depicts the axial load versus the sum of the fastener forces on the second stud from left to right on the sheathed wall-stud model (see Figure 8(a) for distribution across the fasteners). The curve represents a typical magnitude of load carried by the springs, which exceeds 2% of the axial load at peak load. In fact, the comparison between the 2% rule and the FE model are important just to give an idea of fastener demand, since in the FE model the fastener force are magnified where the stud undergoes local buckling (again see Figure 8(a)) and the 2% rule conceptually only takes in account the strength necessary to restrain global buckling in a pinned-pinned column.
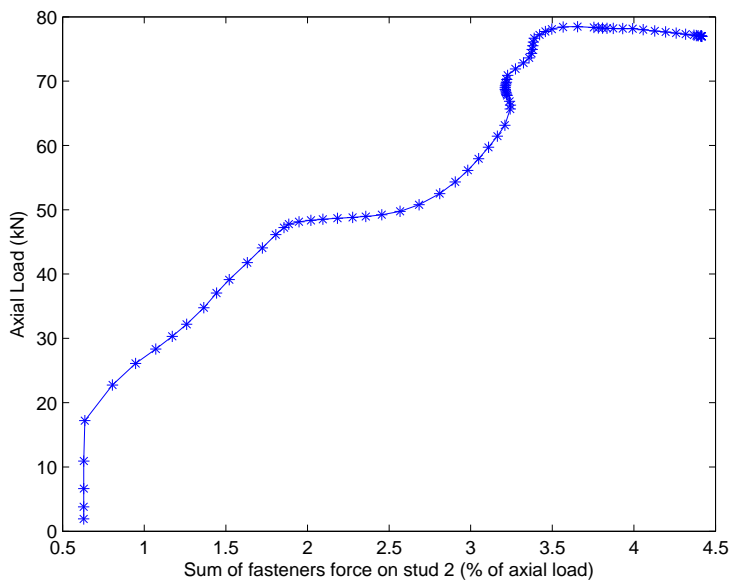

Figure 12: Sum of fasteners force in the k_x spring on second stud (left to right) of sheathed wall-stud (Figure 8(a)) versus axial load.

3 COMPARISON BETWEEN FE MODELS AND ANALYTICAL SOLUTION

For global buckling, the fastener demands can be analytically approximated based on an energy formulation employing beam theory, discrete springs at the bracing locations, and an assumed deformation shape as a Fourier sine series as provided in Vieira and Schafer (2013). A geometric non-linear shell FE model of a 362S162-68 stud, simply supported, with k_x, k_z, k_ϕ springs 305 mm (12 in.) o.c. along the length, is used to verify the analytical solution. It is worth emphasizing that the analytical solution is for global buckling only, hence the fastener forces are only related to restricting global buckling. Purely for verification purposes, to eliminate local and distortional buckling, the stud thickness is changed from 1.67 mm (0.0656 in.) to 6.35 mm (0.25 in.).

Initial imperfections play an important role in determining the fastener demand. If only twist imperfection is applied to the cross-section, the shell FE and the analytical solution for fastener

demand of the center fastener shows similar results, Figure 13(a). If camber imperfection or camber and twist imperfections are applied, the shell FE and the analytical solution may lead to a different prediction of the fastener force, Figure 13(b and c). A better approximation is given if the three buckling modes (minor-axis flexure and the two coupled flexural-torsional modes) of the analytical solution are taken in account to amplify the lateral displacement, Figure 13(d). It is common to consider only the first mode, because in classical flexural buckling the other modes represent only a small contribution to the displaced shape, but in buckling of singly-symmetric studs flexural-torsional, and weak-axis buckling are often at similar elastic buckling values and magnification in both modes as load (P) goes to the buckling load (P_{cr}). For best accuracy in the fastener force prediction it is important to consider the additional buckling modes.
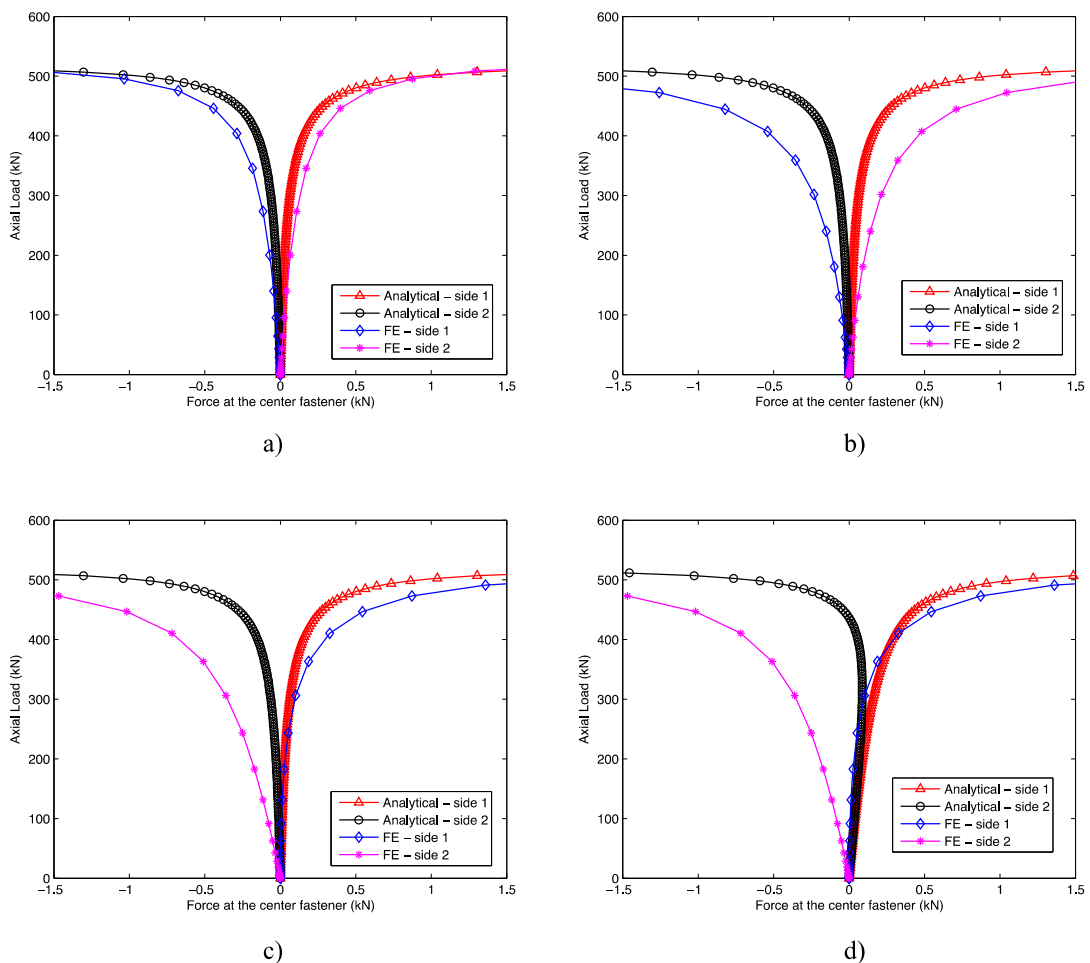

Figure 13: Fastener demand in the x direction. Comparison between FE model and analytical solution of a simple-supported stud of geometry similar to 362S162-68, but thickness of 6.35mm (0.25in.) a) Stud with only twist initial imperfection (twist=1.23^{o}), b) Stud with twist and camber initial imperfection (twist=1.23^{o}, camber=L/2887), c) Stud with all global initial imperfections (twist=1.23^{o}, camber=L/2887, bow=L/1659), d) Stud with all global initial imperfections (twist=1.23^{o}, camber=L/2887, bow=L/1659), and analytical solution considers the displacement due to all three global buckling modes.

The analytical solution is also compared to the OSB-OSB single-column and the full-wall OSB-OSB shell FE model, as depicted in Figure 14. To take in account the clamped-clamped boundary conditions of the model, the analytical solution is found for a buckling length of one half of the actual column height. Even though the shell FE models in this case consider not only global, but also local and distortional initial imperfection, the analytical solution still results is a reasonable prediction of the fastener forces for the wall studs. It is worth noting that the fasteners at mid-height are compared to the analytical solution since this is where first mode global is maximized, but these fasteners are little influenced by local buckling deformations in this case.
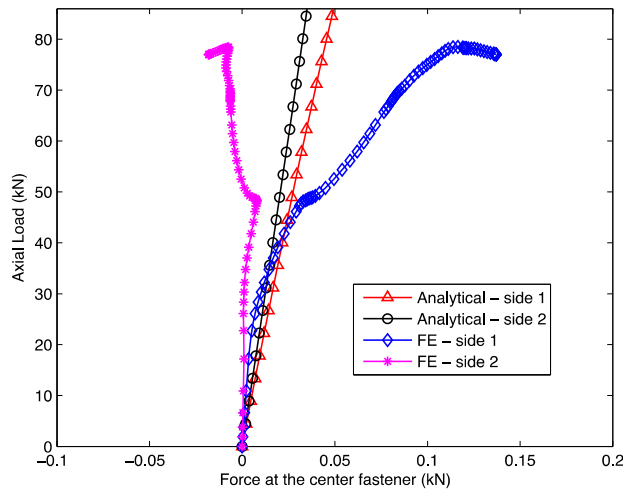

Figure 14: Comparison between FE model and analytical solution considering all the buckling modes
in a wall stud as depicted in Figure 10.

4 STUD-TO-TRACK DEMAND

It was found in the shell FE models that the maximum shear force on the stud-to-track fasteners is approximately 5% of the axial load, but it is worth pointing out again that the FE models consider perfect contact between stud end and track web. More information on this topic may be found in Laboube and Findlay (2007).

5 CONCLUSIONS

Fastener demands developed between sheathing and studs are explored by means of validated shell finite element collapse models of sheathed single studs and sheathed full wall assemblies. In addition to stability of the studs plasticity of the steel, or more specifically the stud-to-track connection, also plays an important role in defining the fastener forces along the length of a sheathed stud. Beneficial redistribution of the fastener demands was observed in the wall stud models until about 85% of the peak load. Beyond 85% of peak load fastener demands in the field studs often do not control and instead fastener demands in the connections in the corners take greater demands, and have less ability to redistribute. Redistribution, however, depends on the extent to which local buckling is

developed at the ends of the field studs and is thus a function of the stud cross-sectional slenderness. Wall stud assemblies with sheathing of very different stiffness; for example oriented strand board (OSB) on one side and bare on the other, may not provide significant restraint, but do not result in fastener demands that exceed wall studs with similar sheathing stiffness (e.g. OSB on both sides). A simple analytical model is shown to reasonably predict the fastener demands, but a better approximation is given if all three buckling modes of the analytical solution are taken in account when amplifying the lateral displacement. The load carried by the springs does exceed the 2% bracing rule necessary to restrain global buckling, but it is shown that the load is magnified where the stud undergoes local buckling.

Acknowledgments

References

ABAQUS, *ABAQUS/Standard Version 6.7-1*, D. Systemes, Editor 2007.

AISI-S200, *North American Standard for Cold-Formed Steel Framing – General Provisions.* American Iron and Steel Institute, 2007.

AISI-S211, *North American Specification for the Design of Cold-Formed Steel Structural Members.* American Iron and Steel Institute, 2007.

Chen, C.Y., A.F. Okasha, and C.A. Rogers, *Analytical Predictions Of Strength and Deflection Of Light Gauge Steel Frame/Wood Panel Shear Walls.* Advances in Engineering Structures, Mechanics & Construction, 2006: p. 381-391.

Fiorino, L., G. Della Corte, and R. Landolfo, *Experimental tests on typical screw connections for cold-formed steel housing.* Engineering Structures, 2007. **29**(8): p. 1761-1773.

Laboube, R.A. and P.F. Findlay, *Wall stud-to-track gap: Experimental investigation.* Journal of Architectural Engineering, 2007. **13**(2): p. 105-110.

Miller, T.H. and T. Pekoz, *Behavior of cold-formed wall stud-assemblies.* Journal of structural engineering New York, N.Y., 1993. **119**(2): p. 641-651.

Okasha, A.F., *Okasha, A.F., Performance of Steel Frame/Wood Sheathing Screw Connections Subjected to Monotonic and Cyclic Loading, 2004, McGill University* in *Civil and Environmental Engineeering*, McGill University: Montreal.

Schafer, B.W. and T. Peköz, *Computational modeling of cold-formed steel: Characterizing geometric imperfections and residual stresses.* Journal of Constructional Steel Research, 1998. **47**(3): p. 193-210.

Schafer, B.W. and V.M. Zeinoddini. *Impact of global flexural imperfections on the cold-formed steel column curve.* in *19th International Specialty Conference on Recent Research and Developments in Cold-Formed Steel Design and Construction.* 2008.

Schafer, B.W., O. Iourio, and L.C.M. Vieira Jr, *Notes on AISI Design Methods for Sheathing Braced Design of Wall Studs in Compression*, in *A supplemental report for AISI-COFS Project on Sheathing Braced Design of Wall Studs,* 2008, The Johns Hopkins University: Baltimore.

Simaan, A. and T.B. Pekoz, *Diaphragm Braced Members and Design of Wall Studs.* ASCE J Struct Div, 1976. **102**(1): p. 77-92.

SSMA, *Product Technical Information - Complies with 2006 IBC*. Steel Stud Manufacturers Association, 2010.

Vieira, L., Jr. and Schafer, B. W. *Behavior and Design of Sheathed Cold-Formed Steel Stud Walls under Compression* in *J. Struct. Eng.* 139, SPECIAL ISSUE: Cold-Formed Steel Structures, 772–786, 2013.

Vieira, L.C.M. ; Shifferaw, Yared ; Schafer, B.W. *Experiments on sheathed cold-formed steel studs in compression* in Journal of Constructional Steel Research, v. 67, p. 1554-1566, 2011.

Vieira, L.C.M.J., *Behavior and Design of Sheathed Cold-Formed Steel Stud Walls under Compression*, Johns Hopkins University: Baltimore. p. 239, 2011.

Winter, G., *Lateral Bracing of Beams and Columns*. Journal of the Structural Division, 1960.